Heliyon 10 (2024) e26248

Contents lists available at ScienceDirect

Heliyon

journal homepage: www.cell.com/heliyon

Research article

Ultrasonic-assisted drilling of cortical and cancellous bone in a comparative point of view

Sousan Pourgiv [a,1], Alireza Mosavar [a,b,1], Nima Jamshidi [a,*], Aminollah Mohammadi [c]

[a] Department of Biomedical Engineering, University of Isfahan, 81746-73441, Iran
[b] Department of Biomechanics, School of Mechanical Engineering, College of Engineering, University of Tehran, 14174-66191, Tehran, Iran
[c] Department of Mechanical Engineering, Isfahan University of Technology, Isfahan, 84156-83111, Iran

ARTICLE INFO

Keywords:
Bone drilling
Ultrasonic-assisted drilling
Conventional drilling
SEM imaging
Osteonecrosis
Finite element analysis

ABSTRACT

Background: During bone drilling, a common procedure in clinical surgeries, excessive heat generation and drilling force can cause damage to bone tissue, potentially leading to failure of implants and fixation screws or delayed healing. With this in mind, the aim of this study was to evaluate the efficiency of ultrasonic-assisted drilling compared to conventional drilling as a potential method for bone drilling.
Methods: This study examined optimal drilling parameters based on previous findings and investigated both cortical and cancellous bone. In addition to evaluating drilling force and temperature elevation, the effects of these factors on osteonecrosis and micro-crack formation were explored in ultrasonic-assisted and conventional drilling through histopathological assessment and microscopic imaging. To this end, three drilling speeds and two drilling feed-rates were considered as variables in the *in vitro* experiments. Furthermore, numerical modeling provided insight into temperature distribution during the drilling process in both methods and compared three different vibration amplitudes.
Results: Although temperature elevations were lower in the conventional drilling, ultrasonic-assisted drilling produced less drilling force. Additionally, the latter method resulted in smaller osteonecrosis regions and did not produce micro-cracks in cortical bone or structural damage in cancellous bone.
Conclusions: Ultrasonic-assisted drilling, which caused less damage to bone tissue in both cortical and cancellous bone, was comparatively more advantageous. Notably, this study demonstrated that to determine the superiority of one method over the other, we cannot rely solely on temperature variation results. Instead, we must consider the cumulative effect of both temperature elevation and drilling force.

1. Introduction

Drilling into bone is a common practice in orthopaedic and prosthodontic surgeries, but conventional drilling can cause

* Corresponding author. Department of Biomedical Engineering, Faculty of Engineering, University of Isfahan, Isfahan, 81746, Iran.
E-mail address: n.jamshidi@eng.ui.ac.ir (N. Jamshidi).
[1] These authors contributed equally to this work.

https://doi.org/10.1016/j.heliyon.2024.e26248
Received 7 May 2022; Received in revised form 30 August 2023; Accepted 8 February 2024
Available online 16 February 2024

considerable thermal and mechanical damages in drilling site [1]. The thermal damages can result in 'thermal osteonecrosis', which is death of bone cells (osteocytes) due to loss of blood supply caused by excessive heat. This is thought to be caused by the force, friction, and heat generated during drilling [2]. Presence of empty osteocyte lacunae is a pathological indicator of this phenomenon. Mechanical damage can also occur due to the force applied during drilling, resulting in micro-cracks in the mineralized bone matrix, which can lead to 'osteocyte apoptosis' [3]. While some micro-cracks may heal during the remodeling process, others can cause damage to the bone structure [4]. Therefore, it is important to carefully control the amount of heat and force generated during drilling, as the success of the surgery depends heavily on these factors. Necrosis and apoptosis of osteocytes can negatively impact 'osseointegration' and the healing process, increasing the risk of implant and screw loosening and failure [5].

To reduce the risk of micro-cracks and thermal osteonecrosis, this *in vitro* study aimed to evaluate the effectiveness of ultrasonic-assisted drilling (also known as 'ultrasonic drilling') in both cortical and cancellous bone, and to compare it with conventional drilling. Ultrasonic drilling is a method that applies high-frequency vibrations (over 20 KHz) to the longitudinal axis of the drilling bit [6]. To compare the two methods, we assessed the control of osteonecrosis through temperature variations and histopathological evaluations, and the control of micro-cracks through measurements of the mean applied force and scanning electron microscope (SEM) evaluations. In addition, experiments were conducted using all combinations of three different drilling feed-rates and two different drilling speeds. Finally, we conducted an *in silico* study using finite element analysis to examine temperature distribution during drilling with both methods. This not only shed light on the experimental results but also allowed us to investigate the effect of vibration amplitude in ultrasonic drilling.

2. Materials and methods

1. Bone Specimens

For *in vitro* drilling, ovine lumbar vertebrae, which has both cortical and cancellous bone regions, was employed. Ovine bone is commonly used in orthopaedic animal-experiments due to its similar properties to human bone [7–10]. According to comparative body of this study, any possible discrepancy in bone properties does not actually affect deductions [5]. Fresh bones were prepared for drilling according to the literature [11]. It is noteworthy to mention that although body blood flow acts as coolant during drilling *in vivo*, its influence is negligible based on literature [12].

2. Drilling of Bone

To compare the two drilling methods under the same drilling conditions, except for the ultrasonic vibrations applied in the ultrasonic method, we designed and implemented a setup consisting of an ultrasonic assembly for drilling, a 4 mm diameter drill bit, a dynamometer (for measuring mean drilling force), and an industrial CNC milling machine (Fig. 1). The ultrasonic assembly provided longitudinal vibration for ultrasonic drilling with optional frequency of 20 KHz and amplitude of 20 μm. Moreover, three drilling speeds of 500, 1200, and 2000 rpm and two drilling feed-rates of 30 and 60 mm per minute were considered [13–15]. Each vertebral bone was drilled using both drilling methods with similar drilling parameters. Furthermore, to ensure the precision and validity of results, each experiment was repeated twice more.

3. Investigation of Temperature Variations

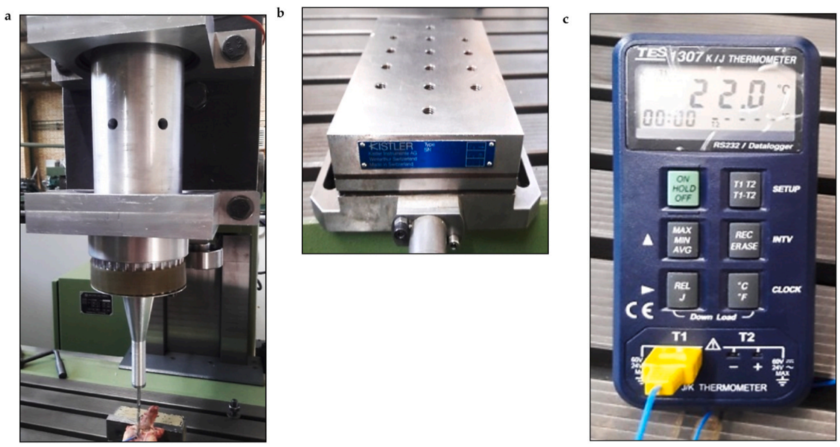

Fig. 1. The experimental setup for drilling of bones that included temperature and force measurements. a) Ultrasonic assembly for drilling; b) Dynamometer; c) Dual-channel data logger (for recording temperatures). The employed CNC milling machine had options for regulation of drill speed and feed-rate. Moreover, the maximum bone temperatures during drilling were measured with two thermocouples.

To record temperature variations during drilling, we used a type K thermocouple [5,16]. The thermocouple was placed 0.5 mm away from the drilling site, and it was inserted to a depth of 10 mm in the bone [5]. The room temperature was 22 °C, and the bones were warmed up to the same temperature.

4. Histopathological and SEM Evaluation

For histopathological study, we first decalcified the specimens in a nitric acid solution. After keeping them in formalin, we prepared one-half of their circular section for SEM imaging, while the second half needed further processing for histopathological evaluation. Therefore, we kept the latter half of each specimen in an alcohol solution for the dehydration process. After employing xylene and paraffin wax, we sliced the specimens with a microtome machine to obtain longitudinal sections of the holes and surrounding tissues. Finally, we used hematoxylin and eosin for staining. To assess osteonecrosis around each hole, we considered the radius of the region in which more than 90% of osteocyte lacunas were empty under an optical microscope.

The first mentioned half of each specimen was considered for examining micro-cracks in the bone. Hence, after a dehydration process, we used a SEM to capture images from the surface of each hole with 80x and 200x magnifications.

5. Finite Element Modeling

To gain a better understanding of our experimental results, we utilized the finite element method for numerically model both drilling methods. Finite element analysis is inherently an approximation tool that can still produce realistic models by employing applicable approximations and simplifications that take important aspects of the problem into account [17,18]. To avoid time-consuming and expensive simulations, we considered 2-dimensional models [19–21] since the chip removal mechanism is identical in 2-dimensional and 3-dimensional models [19]. In our modeling, we considered bone structure as an isotropic elastic-plastic material that was dependent on strain rate, and we used the Johnson-Cook model to define the plastic behavior. The required thermal and mechanical properties of the drill bit (made of 316 L stainless steel) and the bone were obtained from the literature [22–24] (Table 1). We used a linear speed of 400 mm/s according to our experimental drilling speeds. Additionally, we modeled three different amplitudes of 10, 15, and 20 μm for ultrasonic drilling with a vibration frequency of 20 KHz. Finally, the friction coefficient was set to 0.3 for surface-to-surface contacts in the models. Although our simulations aimed to study the temperature distribution pattern in each drilling method, we also investigated the influence of vibration amplitude in ultrasonic drilling.

3. Results

1. Temperature Variations and Drilling Forces

The numerical results of the study are presented in Table 2, which displays the maximum generated temperature and the mean required force during each experiment. To better understand the differences between the drilling methods under various conditions, Fig. 2a and b illustrate the outcomes for temperature and mean force, respectively. These figures indicate that while the feed-rate had minimal impact on temperature rise in conventional drilling, its effect was dramatic in ultrasonic drilling. Additionally, there was a direct relationship between the drilling force and the feed-rate, and an inverse relationship with the drilling speed.

Fig. 3 presents the experimental outcome of the dynamometer, providing insight into the qualitative differences of instantaneous drilling forces between the two drilling methods. As shown in the figure, the drilling duration was 10 s with respect to the feed-rate and drilling depth. Although the force peaked in the both drilling methods while passing through the cortical region of the bones (which is denser and harder than cancellous region as seen in Table 1) [25], the peak was much higher in the conventional drilling. Another notable observation was oscillations in force magnitude during drilling of the cancellous region due to its spongy structure; however, the changes were again higher in conventional drilling.

Table 1
Thermal and mechanical characteristics of the drill bit and the bone.

Characteristic	Drill Bit	Cortical Bone	Cancellous Bone
Density ($Kg.m^{-3}$)	7990	1830	170
Poisson's Ratio	0.25	0.30	0.25
Modulus of Elasticity (MPa)	193×10^3	14×10^3	291
Yield Stress (MPa)	290	110	1.92
Ultimate Stress (MPa)	579	155	2.23
Hardening Modulus (MPa)	–	100	20
Hardening Exponent	–	0.1	1.0
Failure Plastic Strain	–	9.68×10^{-3}	14.5×10^{-3}
Strain Rate Coefficient	–	0.272	0.533
Reference Strain Rate	–	1	1
Specific Heat Capacity ($J.Kg^{-1}.C^{-1}$)	500	1640	1477
Thermal Conductivity ($W.m^{-1}.K^{-1}$)	16.2	0.452	0.087

Table 2
The numerical results of the entire experiments.

Drilling Parameter		Maximum Temperature (°C)		Drilling Force (N)	
Feed-Rate ($mm.min^{-1}$)	Drilling Speed (rpm)	Conventional Drilling	Ultrasonic Drilling	Conventional Drilling	Ultrasonic Drilling
30	500	$25.8^{\pm 0.5}$	$36.7^{\pm 1.4}$	$9.59^{\pm 0.3}$	$3.65^{\pm 0.7}$
30	1200	$25.9^{\pm 1.0}$	$38.9^{\pm 0.9}$	$6.16^{\pm 0.6}$	$3.38^{\pm 0.3}$
30	2000	$28.0^{\pm 1.5}$	$37.1^{\pm 1.3}$	$4.91^{\pm 0.1}$	$2.72^{\pm 0.2}$
60	500	$25.7^{\pm 0.9}$	$27.3^{\pm 0.9}$	$12.23^{\pm 0.9}$	$5.20^{\pm 0.4}$
60	1200	$25.0^{\pm 0.1}$	$29.7^{\pm 0.5}$	$7.15^{\pm 1.1}$	$4.36^{\pm 0.5}$
60	2000	$28.2^{\pm 0.2}$	$29.3^{\pm 0.2}$	$6.28^{\pm 0.3}$	$4.05^{\pm 0.3}$

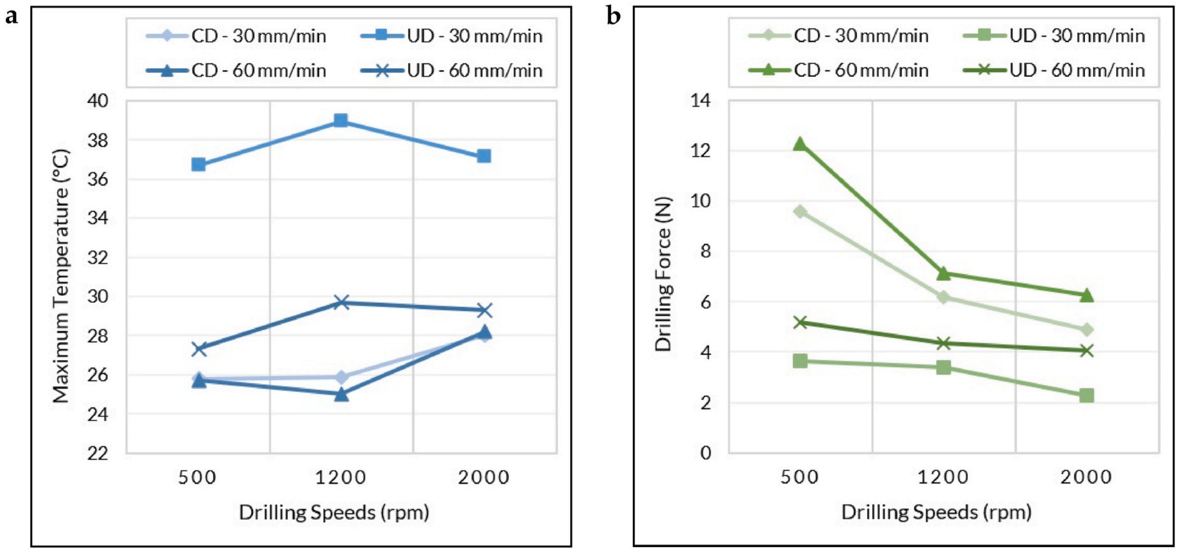

Fig. 2. a) Diagram of recorded maximum temperatures in experiments; b) Diagram of mean drilling forces in experiments. In the diagrams, CD represents conventional drilling method and UD denotes ultrasonic drilling method.

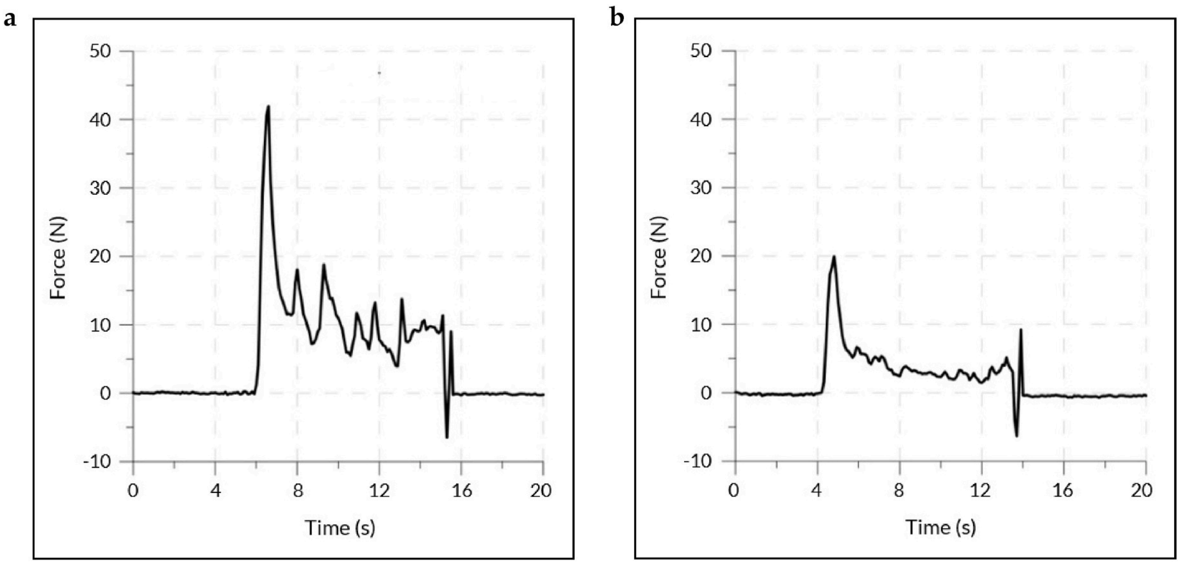

Fig. 3. The experimental force-time diagrams (based on dynamometer outcomes) with drilling speed of 500 rpm and feed-rate of 60 mm min^{-1} for a) the conventional drilling and b) the ultrasonic drilling.

2. Histopathological and SEM Evaluation

Fig. 4 provides an example of our histopathological observations, depicting a region around drilling site with multiple empty osteocyte lacunae. Our observations revealed that the osteonecrosis region was greater in the cortical bone compared to the cancellous bone and was significantly larger in specimens from conventional drilling compared to those from ultrasonic drilling. The largest osteonecrosis region was observed in conventional drilling with a drilling speed of 500 rpm and a feed-rate of 60 mm min^{-1} (Fig. 4), measuring approximately 1.1 mm in the cortical bone and 0.4 mm in the cancellous bone. According to Fig. 2, this specimen had one of the lowest temperature rises but the highest drilling force. While other specimens of conventional drilling had smaller osteonecrosis regions compared to this specimen, particularly in the cortical bone, the amount of osteonecrosis in all of them was higher than that in all specimens of ultrasonic drilling. Notably, the amount of osteonecrosis did not change significantly in the cancellous bone during conventional drilling.

For the ultrasonic drilling, we observed the largest osteonecrosis region in the specimen with a drilling speed of 1200 rpm and a feed-rate of 30 mm min^{-1}, measuring approximately 0.6 mm in the cortical bone and 0.4 mm in the cancellous bone. According to Fig. 2, unlike the aforementioned specimen of conventional drilling, this specimen had one of the lowest drilling forces but the highest temperature rise. However, there was a significant difference in osteonecrosis in the cortical region. Ultimately, the least amount of osteonecrosis, in both cortical and cancellous bone, was observed in one of the specimens of the ultrasonic drilling with a drilling speed of 2000 rpm and a feed-rate of 60 mm min^{-1}. Its osteonecrosis region measured approximately 0.2 mm in both cortical and cancellous bones.

The results of SEM imaging were used to investigate micro-cracks propagation in bone structure. While conventional drilling resulted in multiple micro-cracks in the cortical region and destruction of the cancellous region (Fig. 5a and b), ultrasonic drilling produced no micro-cracks in the cortical bone and preserved the spongy structure of cancellous bone (Fig. 5c and d).

3. Finite Element Analysis

According to the simulations, temperature rise in conventional drilling occurred only in the created chip (Fig. 6a), while in ultrasonic drilling, there was a considerable temperature rise in both the chip and the cutting edge of the bone (Fig. 6b). This difference

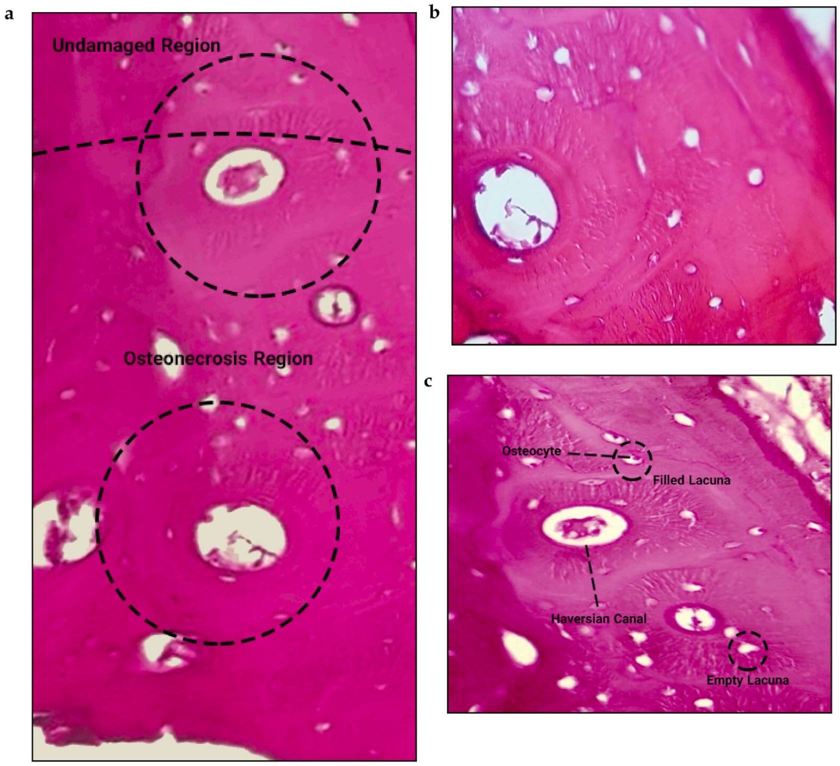

Fig. 4. a) Image of bone tissue in 100 × magnification around drilling site in the specimen of cortical bone in the conventional drilling with drilling speed of 500 rpm and feed-rate of 60 mm min^{-1}. The drilling edge is on the inferior side of this image and a crossed line shows the osteonecrosis region. On the superior side of this image, less than 90% of osteocyte lacunae are empty. In this figure, in addition to osteocyte lacunae, some Haversian canals are observed. b) Image of bone tissue in 400 × magnification from the osteonecrosis region with lots of empty lacunae. c) Image of bone tissue in 400 × magnification from the region between empty lacunae and undamaged osteocytes. Empty lacuna, filled lacuna, Osteocyte in lacuna, and Haversian canal are labeled on the figure.

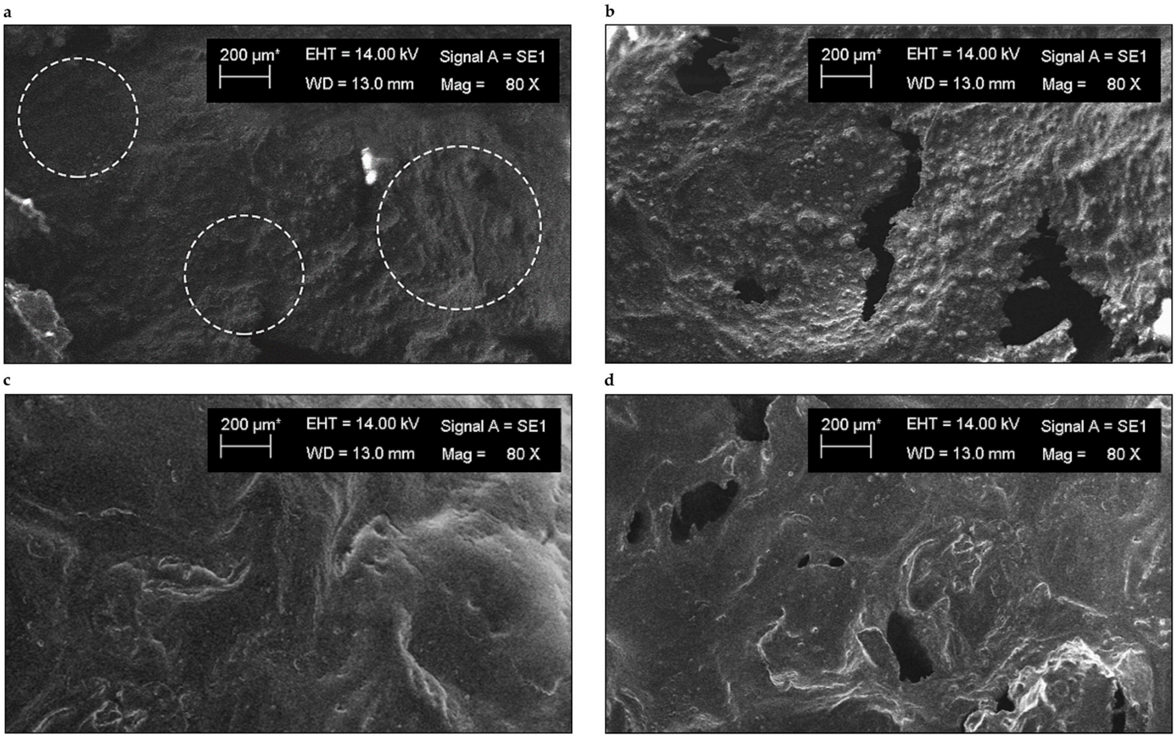

Fig. 5. a) SEM image of bone surface around drilling site in the conventional drilling method for the specimens with drilling speed of 500 rpm and feed-rate of 60 mm min^{-1} in 80 × magnification, in the cortical bone that micro-cracks can be seen, and b) in its cancellous bone that the spongy structure was ruined. c) SEM image of bone surface around drilling site in the ultrasonic drilling method for the specimens with drilling speed of 1200 rpm and feed-rate of 30 mm min^{-1} in 80 × magnification, in the cortical bone, and d) in the related cancellous bone. In this figure the spongy structure is maintained.

in the temperature distribution between the two methods, observed in both cortical and cancellous bone models, can explain the difference in recorded maximum temperatures around the drilling site during experiments. In fact, the temperature rise in the cutting edge could have a greater impact on recorded temperature since it remained in the bulk bone.

Furthermore, increasing the vibration amplitude from 10 to 15 and then to 20 μm resulted in an increase in both temperature rise and temperature distribution in the cutting edge of the bone (Fig. 6c and d). On the other hand, when comparing the required force under these three conditions, we observed that it decreased with increasing amplitude, while all were lower than the force required in conventional drilling simulation.

4. Statistical Analyses

To determine the influence of drilling methods and their parameters (the factors) on the mean drilling force and temperature (the outcomes), we conducted an analysis of variance (ANOVA) to assess the significance of each individual factor and their interaction on the outcomes. As shown in Table 3, *F*- and *P*-value indicate that the effect of all three factors on force and temperature was significant (*P*-value ≤0.05). While the drilling method was the most influential factor on both outcomes (with the highest contribution), drilling speed had a completely different level of effectiveness on them. Despite having a negligible influence on temperature, drilling speed had a considerable impact on force. In terms of feed-rate, it not only had a very high effect on temperature but also contributed significantly to force. This table shows that in both drilling methods, force had a direct relationship with feed-rate and always increased with its increase. According to 2-way interactions, only the interaction between the drilling method and speed had a significant effect on the force, while the most influential interaction for temperature was between the drilling method and the feed-rate.

4. Discussion

Recent literature has shown an increasing interest in studying the efficiency of ultrasonic drilling in bone [6,14,15,26–31]. However, each study utilized its own drilling parameters, resulting in specific outcomes. Furthermore, previous studies have only the application of ultrasonic drilling in cortical bone. In this study, we considered optimum drilling parameters based on previous findings and examined both cortical and cancellous bone. Additionally, we investigated not only the drilling force [6,26,28] and temperature rise [14,15,27–31], but also assessed their effects on necrosis and apoptosis of osteocytes through histopathologic evaluation [14,15], as well as micro-cracks propagation and mechanical damages using SEM imaging. Finally, by employing finite element modeling, we

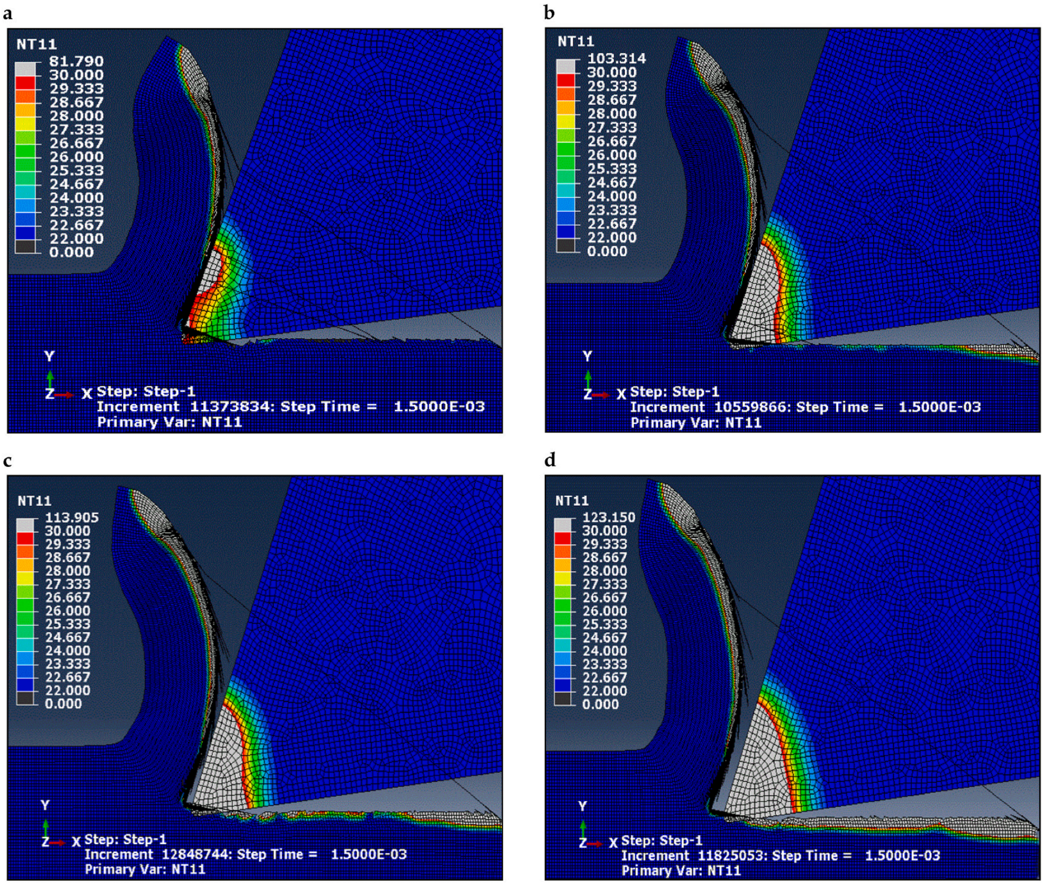

Fig. 6. Temperature distribution in the cutting edge and the drilled chip of cortical bone in a) the conventional drilling method, and in the ultrasonic drilling method with vibration amplitudes of b) 10 μm, c) 15 μm, and d) 20 μm.

Table 3
The results of statistical analyses (ANOVA) for the entire experiments. In the table the following codes are used; DM for drilling method, FR for feed-rate (mm.min^{-1}), and DS for drilling speed (rpm).

Source	Analyses for the Force			Analyses for the Temperature		
	Contribution	F-Value	P-Value	Contribution	F-Value	P-Value
Model	96.62%	82.64	0.000	96.58%	81.57	0.000
Linear	83.38%	160.45	0.000	74.10%	140.80	0.000
DM	50.58%	389.30	0.000	49.41%	375.58	0.000
FR	7.52%	57.92	0.000	22.36%	169.96	0.000
DS	25.28%	97.29	0.000	2.32%	8.83	0.001
2-Way Interactions	13.24%	20.38	0.000	22.48%	34.18	0.000
DM × FR	0.12%	0.94	0.342	19.61%	149.04	0.000
DM × DS	12.38%	47.63	0.000	2.59%	9.83	0.001
FR × DS	0.74%	2.85	0.076	0.29%	1.10	0.347

gained insight into the temperature distribution during each drilling method.

With regard to the temperature, many previous studies on ultrasonic drilling in bone have focused solely on determining temperature changes [27,29–31] as its elevation is considered an indicator for osteonecrosis [2,32]. However, studies comparing ultrasonic drilling and conventional drilling based on temperature elevation have yielded inconsistent results. Alam et al. [27] studied ultrasonic drilling with a frequency range of 5–30 KHz and found that temperatures were lower for frequencies below 20 KHz compared to conventional drilling with the same drilling parameters. In contrast, our results using a frequency of 20 KHz were in stark contrast to this outcome, with the contrast being more significant at lower feed-rates (Fig. 2a). Furthermore, they claimed that vibration amplitude did not affect temperature rise, which contradicts the results of our finite element analysis. Similar contrary views are also present in other studies [14,26,29]. Despite these inconsistencies, there is also support for our results on the comparison of temperature elevation in the literature [15,30,31]. As our finite element analyses also suggested, the temperature distribution differed between the two drilling methods, which may explain the higher temperature elevation in ultrasonic drilling. Bai et al. [31] proposed that in this method, the superposed motion intensifies friction at the interface between the drill body and the wall of the bone hole, leading to intensive heat generation.

Regarding the mean force, our results on the efficacy of ultrasonic drilling compared to conventional drilling (Fig. 2b) were consistent with previous studies [6,28]. It has been suggested that ultrasonic drilling results in lower drilling force and torque compared to conventional drilling by altering the mechanism of chip formation [6]. Shakouri et al. [28] reported similar findings for a drilling speed of 1000 rpm. However, in their study, the temperature rise for ultrasonic drilling with a drilling speed of 2000 rpm was negligible and independent of feed-rate, which contradicts our results.

When comparing Fig. 2a with Fig. 2b, we can explain the observed trends as follows: increasing the feed-rate increases friction, resulting in a higher mean force and greater heat generation. However, as the feed-rate increases, drilling time decreases, leading to lower heat transmission to the bone and reduced temperature elevation. On the other hand, as the drilling speed increases, the amount of frictional energy generated by the drill bit also increases. Since most of the drilling energy is converted to heat, increasing the rotational speed raises the temperature of the bone [33].

As shown in Fig. 2a, the effect of feed-rate on temperature was more pronounced in ultrasonic-assisted drilling as compared to conventional drilling. According to the literature, ultrasonic drilling generates a larger amount of heat compared to conventional drilling due to its extremely high axial velocity [31]. This was observed in our experiments with a feed-rate of 30 mm/min. However, increasing the feed-rate not only decreases drilling time, which affects heat generation, but also reduces the time for heat transfer from the cutting edge to the bulk bone. Our numerical study showed a difference in temperature distribution between the two methods. In ultrasonic drilling, there is considerable heat transfer from the cutting edge of the bone to the bulk. As a result, when we increased the feed-rate for this method, there was less time for heat transfer in the bulk. Consequently, at higher feed-rates, the recorded temperature was closer to that of conventional drilling.

The attention-grabbing comparative point in the results, particularly in the diagrams of Fig. 2, is that while we found lower temperature elevation for conventional drilling, ultrasonic drilling had better results for drilling force. However, the primary concern in application is not temperature elevation or force, but rather their effects on osteonecrosis and mechanical damage. As previously mentioned, the finding that conventional drilling had an advantage in terms of temperature elevation could indicate less osteonecrosis compared to ultrasonic drilling, particularly at a feed-rate of 30 mm. min-1. However, the finding that ultrasonic drilling was more competitive in terms of required force raises doubts about the superiority of conventional drilling, as it is believed that osteonecrosis is caused by drilling force and friction and that mechanical damage due to applied force can cause osteocyte apoptosis. Additionally, the cumulative effect of force magnitude and temperature rise is unclear. Therefore, our histopathologic observations, as explained in the results section, were particularly interesting, especially since they were supported by SEM imaging. We can conclude that ultrasonic drilling was comparatively more advantageous based on bone damage in both cortical and cancellous bone. The results showed that death of osteocytes was due to both temperature elevation and drilling force, and both parameters should be considered when assessing bone damage. This is consistent with some previous findings in the literature [15,34].

Further *in vivo* studies on the clinical success of ultrasonic drilling are needed, both in animals and humans. To reach a more conclusive understanding, consideration of additional drilling parameters may be helpful, and a delamination study of the drilled holes for both drilling methods could be carried out. Microstructural analysis and calculation of the delamination percentage in the delamination zones for both methods will aid in determining the superiority between the drilling methods.

5. Conclusion

This study provided a novel understanding of the efficiency of ultrasonic-assisted drilling in cortical and cancellous bone by evaluating the effects of drilling force and temperature rise on necrosis and apoptosis of osteocytes, as well as micro-cracks propagation and mechanical damage. A comparison between ultrasonic-assisted drilling and conventional drilling revealed that, although the latter method resulted in lower temperature elevations, the former method had lower drilling forces. In conclusion, based on our observations of bone tissue histopathology and SEM imaging of the drilling surface, ultrasonic-assisted drilling was comparatively more advantageous.

List of abbreviations

Not applicable.

Ethics approval and consent to participate

Not applicable.

Consent for publication

Not applicable.

Availability of data and material

All data generated or analyzed during this study are included in this published article.

Funding

There was not funding available for this study.

Declaration of competing interest

The authors declare that they have no competing interests.

Acknowledgements

The authors declared no acknowledgements related to this study.

References

[1] F.G. Draenert, R. Mathys Jr., M. Ehrenfeld, Y. Draenert, K. Draenert, Histological Examination of drill sites in bovine rib bone after grinding in vitro with eight different devices, Br. J. Oral Maxillofac. Surg. 45 (2007) 548–552.
[2] F. Karaca, B. Aksakal, Effects of various drilling parameters on bone during implantology: an in vitro experimental study, Acta Bioeng. Biomech. 15 (2013) 25–32.
[3] B. Noble, Bone microdamage and cell apoptosis, Eur. Cell. Mater. 6 (2003) 46–56.
[4] V. Gupta, P.M. Pandey, V.V. Silberschmidt, Rotary ultrasonic bone drilling: improved pullout strength and reduced damage, Med. Eng. Phys. 41 (2017) 1–8.
[5] M.R. Effatparvar, N. Jamshidi, A. Mosavar, Appraising efficiency of OpSite as coolant in drilling of bone, J. Orthop. Surg. Res. 15 (2020) 197.
[6] K. Alam, A. Mitrofanov, V.V. Silberschmidt, Experimental investigations of forces and torque in conventional and ultrasonically-assisted drilling of cortical bone, Med. Eng. Phys. 33 (2011) 234–239.
[7] S. Wan, W. Lei, Z. Wu, D. Liu, M. Gao, S. Fu, Biomechanical and histological evaluation of an expandable pedicle screw in osteoporotic spine in sheep, Eur. Spine J. 19 (2010) 2122–2129.
[8] M.E. Yurttutan, R. Kestane, A. Keskin, O. Dereci, Biomechanical evaluation of oversized drilling on implant stability-an experimental study in sheep, J. Pakistan Med. Assoc. 66 (2016) 147–150.
[9] C.D. Lopez, A.M. Alifarag, A. Torroni, N. Tovar, J.R. Diaz-Siso, L. Witek, E.D. Rodriguez, P.G. Coelho, Osseodensification for enhancement of spinal surgical hardware fixation, J. Mech. Behav. Biomed. Mater. 69 (2017) 275–281.
[10] J.A. McGovern, M. Griffin, D.W. Hutmacher, Animal models for bone tissue engineering and modelling disease, Disease Models and Mechanisms 11 (2018) dmm033084.
[11] W. Wang, Y. Shi, N. Yang, X. Yuan, Experimental analysis of drilling process in cortical bone, Med. Eng. Phys. 36 (2014) 261–266.
[12] G. Augustin, T. Zigman, S. Davila, T. Udilljak, T. Staroveski, D. Brezak, S. Babic, Cortical bone drilling and thermal osteonecrosis, Clin. BioMech. 27 (2012) 313–325.
[13] G. Augustin, S. Davila, K. Mihoci, T. Udiljak, S.D. Vedrina, A. Antabak, Thermal osteonecrosis and bone drilling parameters revisited, Arch. Orthop. Trauma Surg. 128 (2008) 71–77.
[14] G. Singh, V. Jain, D. Gupta, A. Sharma, Parametric effect of vibrational drilling on osteonecrosis and comparative histopathology study with conventional drilling of cortical bone, Proc. Inst. Mech. Eng., Part H 232 (2018) 975–986.
[15] K. Alam, A. Al-Ghaithi, S. Piya, A. Saleem, In-vitro experimental study of histopathology of bone in vibrational drilling, Med. Eng. Phys. 67 (2019) 78–87.
[16] S. Sezek, B. Aksakal, F. Karaca, Influence of drill parameters on bone temperature and necrosis: a fem modelling and in vitro experiments, Comput. Mater. Sci. 60 (2012) 13–18.
[17] A. Mosavar, A. Ziaei, M. Kadkhodaei, The effect of thread design on stress distribution in a dental threaded implant under consideration of bone anisotropy and different osseointegration conditions: a finite element analysis, Int. J. Oral Maxillofac. Implants 30 (2015) 1317–1326.
[18] A. Mosavar, S.R. Hashemi, M. Nili, M. Kadkhodaei, A comparative analysis on two types of oral implants, bone-level and tissue-level, with different cantilever lengths of fixed prosthesis, J. Prosthodont. 26 (2017) 289–295.
[19] K. Alam, A. Mitrofanov, V.V. Silberschmidt, Thermal analysis of orthogonal cutting of cortical bone using finite element simulations, Int. J. Exp. Comput. BioMech. 1 (2010) 236–251.
[20] K. Alam, A. Mitrofanov, V.V. Silberschmidt, Finite element analysis of forces of plane cutting of cortical bone, Comput. Mater. Sci. 46 (2009) 738–743.
[21] C. Santiuste, M. Rodríguez-Millán, E. Giner, H. Miguélez, The influence of anisotropy in numerical modeling of orthogonal cutting of cortical bone, Compos. Struct. 116 (2014) 423–431.
[22] E. Wagnac, P.J. Arnoux, A. Garo, C.E. Aubin, Finite element analysis of the influence of loading rate on a model of the full lumbar spine under dynamic loading conditions, Med. Biol. Eng. Comput. 50 (2012) 903–915.
[23] M. El-Rich, P.J. Arnoux, E. Wagnac, C. Brunet, C.E. Aubin, Finite element investigation of the loading rate effect on the spinal load-sharing changes under impact conditions, J. Biomech. 42 (2009) 1252–1262.
[24] Y.C. Chen, Y.K. Tu, Y.J. Tsai, Y.S. Tsai, C.Y. Yen, S.C. Yang, C.K. Hsiao, Assessment of thermal necrosis risk regions for different bone qualities as a function of drilling parameters, Comput. Methods Progr. Biomed. 162 (2018) 253–261.
[25] Z. Li, D. Yang, W. Hao, T. Wu, S. Wu, X. Li, A novel technique for micro-hole forming on skull with the assistance of ultrasonic vibration, J. Mech. Behav. Biomed. Mater. 57 (2016) 1–13.
[26] K. Alam, M. Khan, V.V. Silberschmidt, Analysis of forces in conventional and ultrasonically assisted plane cutting of cortical bone, Proc. Inst. Mech. Eng., Part H 227 (2013) 636–642.
[27] K. Alam, V.V. Silberschmidt, Analysis of temperature in conventional and ultrasonically-assisted drilling of cortical bone with infrared thermography, Technol. Health Care 22 (2014) 243–252.
[28] E. Shakouri, M.H. Sadeghi, M.R. Karafi, M. Maerefat, M. Farzin, An in vitro study of thermal necrosis in ultrasonic-assisted drilling of bone, Proc. Inst. Mech. Eng., Part H 229 (2015) 137–149.
[29] Q. Zheng, L. Xia, X. Zhang, C. Zhang, Y. Hu, Reduction thermal damage to cortical bone using ultrasonically-assisted drilling, Technol. Health Care 26 (2018) 843–856.
[30] Z. Sun, Y. Wang, K. Xu, G. Zhou, C. Liang, J. Qu, Experimental investigations of drilling temperature of high-energy ultrasonically assisted bone drilling, Med. Eng. Phys. 65 (2019) 1–7.
[31] X. Bai, S. Hou, K. Li, Y. Qu, T. Zhang, Experimental investigation of the temperature elevation in bone drilling using conventional and vibration-assisted methods, Med. Eng. Phys. 69 (2019) 1–7.

[32] T. Udiljak, D. Ciglar, S. Skoric, Investigation into bone drilling and thermal bone necrosis, Advances in Production Engineering and Management 2 (2007) 103–112.
[33] J. Lee, C.L. Chavez, J. Park, Parameters affecting mechanical and thermal responses in bone drilling: a review, J. Biomech. 71 (2018) 4–21.
[34] F. Karaca, B. Aksakal, M. Kom, Influence of orthopaedic drilling parameters on temperature and histopathology of bovine tibia: an in vitro study, Med. Eng. Phys. 33 (2011) 1221–1227.